Modelling of the deposition of molybdenum on silicon from molybdenum hexafluoride and hydrogen

JOURNAL DE PHYSIQUE IV
Colloque C5, supplément au Journal de Physique II, Volume 5, juin 1995

Modelling of the Deposition of Molybdenum on Silicon from Molybdenum Hexafluoride and Hydrogen

E.N. Orij, M.H.J.M. de Croon and G.B. Marin

Eindhoven University of Technology, Laboratorium voor Chemische Technology, P.O. Box 513, 5600 MB Eindhoven, The Netherlands

Abstract: The deposition of molybdenum on silicon from MoF_6 and H_2 is studied using a microbalance setup. The deposition rate is time dependent, which is explained by the significant contribution of the reduction of MoF_6 by Si. A model taking into account both deposition routes and in particular diffusion of Si through the growing layer allows to describe the observations quantitatively. The relative importance of two routes was assessed and the kinetics of the reduction by H_2 could be distinguished from the overall growth kinetics. A partial reaction order of 1.4 in hydrogen was found for the reduction of MoF_6 by H_2. The order in MoF_6 is negative.

1. INTRODUCTION

The low pressure chemical vapour deposition of molybdenum and tungsten from molybdenum hexafluoride and tungsten hexafluoride provides a relatively low-temperature process for use in VLSI-level metallization. Although molybdenum has similar characteristics, W-LPCVD has received much more attention in the last decade: only a few studies report about the reduction of MoF_6 by hydrogen and/or silicon [1-5]. Lifshitz *et al.* [1,2] and Woodruff and Sanchez-Martinez [3] reported a non-self-limiting growth for the reduction of MoF_6 by Si at 448-673 K and 26-120 Pa. Constant deposition rates in time for the reduction of MoF_6 by Si and H_2 were observed at 473-573 K and 26-120 Pa [2], which were described by overall reactions **r.I** and **r.II**

$$2MoF_6(g) + 3Si(s) \rightarrow 2Mo(s) + 3SiF_4(g) \qquad \textbf{(r.I)}$$

$$MoF_6(g) + 3H_2(g) \rightarrow Mo(s) + 6HF(g) \qquad \textbf{(r.II)}$$

Sahin *et al.* studied the deposition of molybdenum by reduction of MoF_6 by Si [4] and H_2 [5] at 120-1300 Pa and 523-673 K. They observed a self-limiting reduction reaction by Si, similar to the reduction of WF_6 by Si [7,8]. Self-limiting thicknesses of 30-130 nm at 130 Pa (MoF_6/He=1/3) and 523-673 K were found. The deposition of molybdenum was 100 % selective in the sense that no growth occurred on silicon oxide. The deposited layers showed extreme porosities of about 30 %, and high and uniform concentrations of oxygen throughout the layers.

This work reports on an *in situ* study on the kinetics of the deposition of molybdenum on silicon from

MoF_6 and H_2 using a microbalance setup. The major objective of this study is to measure the reaction rate of the reduction of MoF_6 by H_2 in the presence of the reduction of MoF_6 by Si.

2. EXPERIMENTAL

The microbalance LPCVD setup is designed to allow *in situ* measurements of the intrinsic deposition rates, i.e. the deposition rate can be monitored during the growth of the layer and the observed rate is not determined by transport phenomena in the fluidum phase. It is depicted schematically in figure 1a.

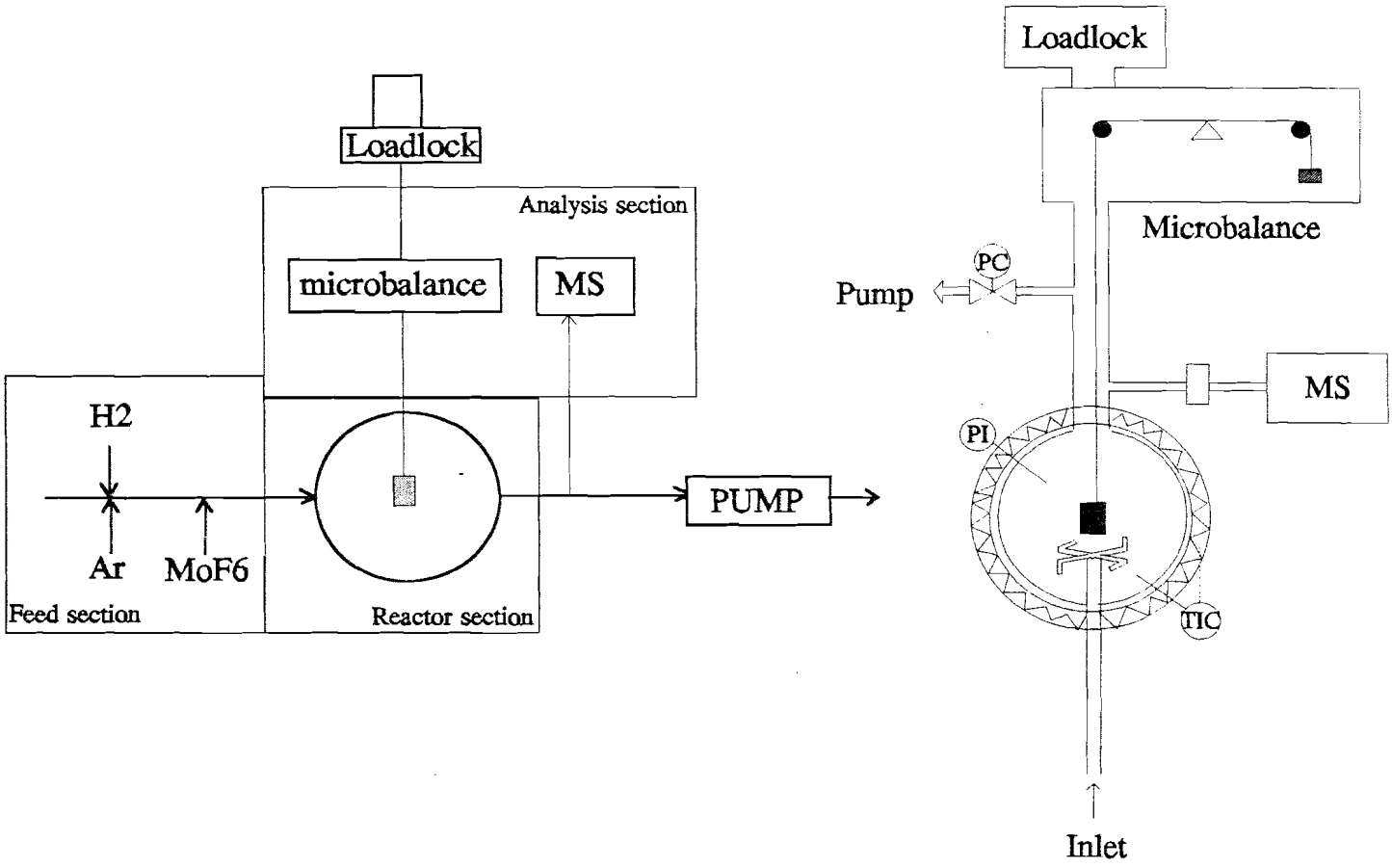

Figure 1a,b Schematic diagrams of the microbalance LPCVD setup (a), and of the reactor section (b).

In the feed section the gas mixture fed to the reactor is prepared. Reactant gas hydrogen (6.0, Air Products) and inert dilutant argon (6.0, Air Products) are mixed with molybdenum hexafluoride (3.0, Cerac) prior to introduction into the reactor. Nitrogen (6.0, Air Products) is used as purge gas. The flow rates of the H_2, Ar and N_2 gases are adjusted by mass flow controllers in a range varying from 2 to 100 sccm. The flow rate of MoF_6 is adjustable from 1 to 20 sccm.

The reactor section consists of a hot wall quartz spherical continuous flow reactor as outlined in figure 1b. Spherical geometry was chosen because it favours mixing and uniformity of heat transfer [9]. The feed mixture is injected through four nozzles of a cross-shaped injector, located just below the centre of the reactor. The nozzles are placed midway between the centre of the reactor and the wall, in two orthogonal planes. The diameters of the reactor ($6.0\ 10^{-2}$ m) and nozzles ($1.8\ 10^{-4}$ m) are chosen on the basis of hydrodynamic relations for axially symmetrical jets as proposed by David and Matras [10] to ensure good mixing. In the middle of the reactor a 15x10 mm^2 sized sample cut from double side polished (100) oriented silicon wafers is suspended from a microbalance by a 0.1

mm diameter NiCr wire. The substrates are cleaned in boiling concentrated HNO_3 (65 %). Prior to the deposition experiments the samples receive a buffered hydrogen fluoride dip in order to remove native silicon oxide from the surface. The silicon substrates are introduced into the reactor via a loadlock. The reactor temperature is measured with a chromel-alumel (K-type) thermocouple in a thermowell located near the silicon sample. The temperature can be set between 450 and 1100 K, and the pressure between 10 and 400 Pa. The leak rate of the system was determined after at least a night of pumping, purging and baking the system, followed by measuring the pressure increase of the isolated system starting from $2 \cdot 10^{-3}$ Pa. The leak rate amounted to about $1 \cdot 10^{-4}$ sccm.
The microbalance (Cahn D-200) is operated in the weight range of 0 to 20 mg. The quadrupole mass spectrometer is coupled to the reactor through an orifice with a diameter of 20 μm, and is used for a qualitative analysis of the gas phase at the outlet of the reactor.
Kinetic experiments were performed at a temperature of 600 K and total pressures from 30 to 200 Pa. Inlet partial pressures of the reactant gases varied from 2.5 to 15 Pa for MoF_6 and from 25 to 100 Pa for H_2.
Grown layers were characterized *ex situ* using SEM, XRD and XPS. The density of the molybdenum films was determined from the film thicknesses measured with SEM and the weight differences of the samples after dissolution of the molybdenum in boiling concentrated H_2SO_4.

3. RESULTS AND DISCUSSION

3.1 Microbalance results

Figure 2 presents the results of a typical experiment. The mass increase is reported per geometric surface area of the sample. In contrast to the results presented by Lifshitz *et al.* [2] a non-linear dependence of the film thickness on time is observed. The deposition rates do not become constant, even not after 30 minutes when a thickness of typically 3 μm is reached. The mass spectrometer spectra show main product peaks at m/e=85 and m/e=20, corresponding to SiF_4 and HF respectively. This is consistent with overall reactions **r.I** and **r.II**.

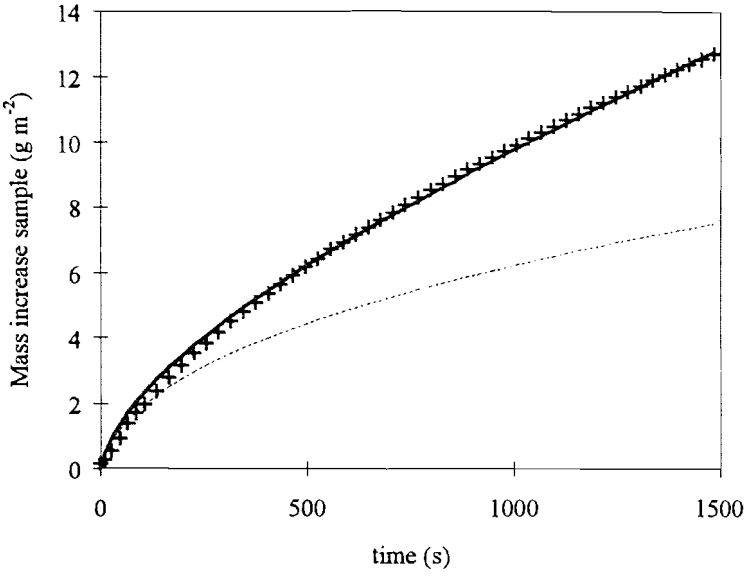

Figure 2. A typical mass versus time curve, + experimental, —— calculated with the model in 3.3 ($D_{Si,eff}=2.08\pm0.01 \cdot 10^{-15}$ m^2 s^{-1}; $k_I'=2.59\pm0.11 \cdot 10^{-8}$ m s^{-1}; $r_{II}=3.70\pm0.02 \cdot 10^{-5}$ mol m^{-2} s^{-1}). --- calculated contribution of **r.I**. Conditions: T=600 K; p°_{H2}= 75 Pa; p°_{MoF6}= 5 Pa; p°_{Ar}= 0 Pa.

Attempts were made to study both reactions separately by depositing molybdenum by reduction of MoF_6 by Si in the absence of H_2 and by reduction of MoF_6 by H_2 in the absence of Si, using other types of surfaces. However the reduction of MoF_6 by Si solely was irreproducible, while attempts to grow on other types of surfaces, like sputtered Pt, sputtered Mo, LPCVD-W and sputtered Ti lead to no growth at all, severe etching, or the same type of time dependent deposition rates as found for Mo-CVD on Si.

3.2 Film characteristics

XRD patterns exhibit only crystalline molybdenum in the deposited layer (figure 3), while from SEM photographs it can be concluded that the layer consists of polycrystalline material with grain sizes of about 0.1 μm (figure 5). The density of the layers amounted to about 70 % of the density of bulk molybdenum, which equals the density found by Lifshitz *et al.* [1,2]. XPS measurements on a molyb-

denum film with a thickness of even 5 μm showed a small amount of Si in the upper atomic layers of the deposited molybdenum (figure 4). The binding energy of 104 eV in the Si 2*p* spectrum corresponds to silicon oxide, which is probably formed during transport of the sample to the XPS apparatus.

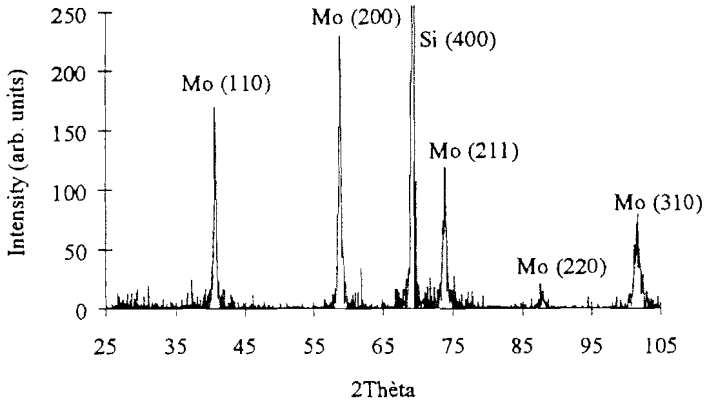

Figure 3. CuKα1-XRD of a CVD grown Mo layer (T = 600 K; p°_{MoF6} = 5 Pa; p°_{H2} = 75 Pa).

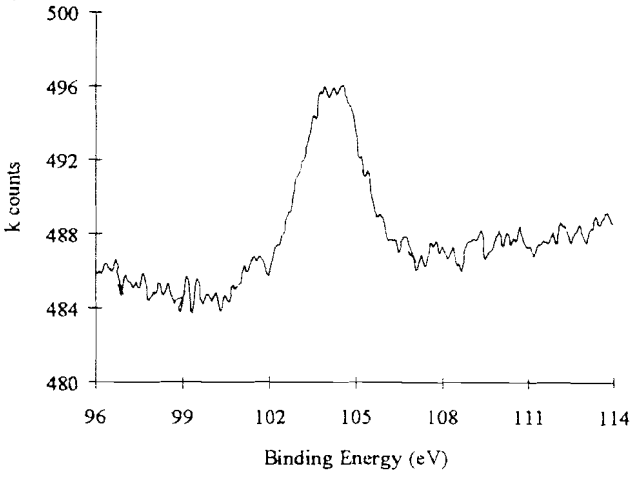

Figure 4. XPS spectrum of the Si 2*p* region of the surface of a Mo layer (T=600 K; p°_{MoF6}=10 Pa; p°_{H2}=50 Pa).

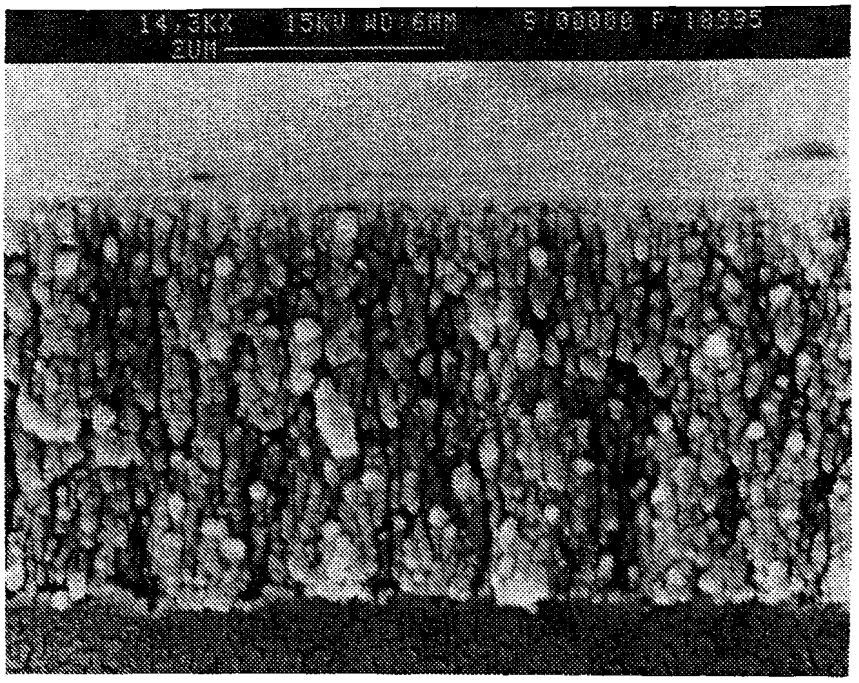

Figure 5. SEM photograph of a typical Mo layer grown at 600 K, p°_{MoF6}= 5Pa and p°_{H2}= 50 Pa during 3000 s.

3.3 Model equations

The time dependent growth behaviour of molybdenum by the reduction of MoF_6 by Si and H_2 can be explained by a model which takes into account the diffusion of elemental Si through the growing molybdenum layer at a finite rate. As the layer grows, the diffusion length of Si increases, leading to a

decreasing Si concentration on the reacting surface and correspondingly to a decrease of the rate of reaction **r.I**, if the reactions are assumed to take place at the external gas-solid interface. As the mass versus time curve in a typical experiment still deflects after even 1500 s (figure 2), reaction **r.I** may be expected to play a significant role in the deposition process. This model is also consistent with the Si in the upper atomic layers observed with XPS and the Si profile through grown molybdenum layers observed by Lifshitz *et al* using SIMS [1]. The observed low density can then, at least partially, be explained by the large amounts of Si in the layer. Diffusion of MoF_6 and/or H_2 through the growing layer is not considered.

Figure 6 shows a schematic presentation of the model which is applied to account for contributions of both reactions **r.I** and **r.II** and, hence, allows to study the dependence of the reduction of MoF_6 by H_2 on the reaction conditions. The properties of the grown layer, the temperature at the surface, and the gas phase concentrations of the reactants at the surface are assumed to be constant in time. Low conversions of the reactants (<15 %) indicate differential operation of the reactor, so the bulk gas phase concentrations are considered equal to the inlet concentrations. Ignoring mass transfer limitations is allowed because of the low Damkohler II number ($r_{obs}L/D_{MoF6}C_{MoF6}$), which is equal to the time scale of transport compared to the time scale of surface reaction; even when the former is based on the reactor radius L, $Da_{II} < 0.05$.

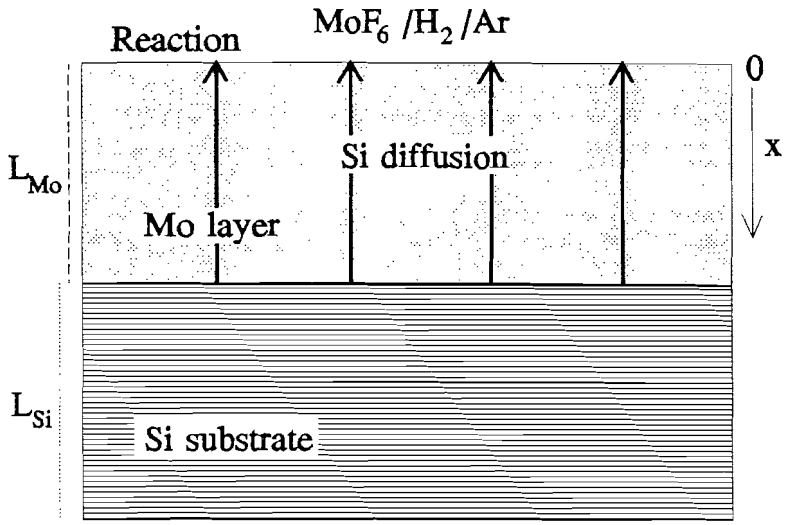

Figure 6. Schematic presentation of the model.

The quantity measured with the microbalance is equal to the net mass increase of the sample, Δm, which is a summation of the production of molybdenum minus the consumption of Si:

$$\frac{\Delta m}{A} = L_{Mo}\rho_{Mo} - (L_{Si,0} - L_{Si})\rho_{Si} \qquad (1)$$

where A is the substrate area, L_{Mo} and $L_{Si,0}$-L_{Si} are the thicknesses of the produced molybdenum layer and consumed Si respectively, and ρ_{Mo} and ρ_{Si} are the densities of the molybdenum and silicon.
The thickness of the molybdenum layer can be calculated from the molybdenum mass balance:

$$\frac{\rho_{Mo}}{M_{Mo}} \frac{dL_{Mo}}{dt} = r_I + r_{II} \qquad (2)$$

with initial condition $L_{Mo}=0$ and $r_I=\frac{2}{3}k_1'C_{Si}|_0$. A first order dependency in the concentration of elemental Si at the surface, $C_{Si}|_0$, is assumed for the reduction reaction by Si. The factor $\frac{2}{3}$ accounts for the reaction stoichiometry. As the gas phase concentrations above the surface are constant during an experiment, the pseudo first order reaction coefficient of the reduction by Si, k_1' (m s^{-1}), and the reaction rate of reaction **r.II**, r_{II} (mol m^{-2} s^{-1}), which both depend on these gas phase concentrations only, will also remain constant during this experiment.The thickness of the consumed Si is obtained from the silicon mass balance:

$$\frac{\rho_{Si}}{M_{Si}} \frac{d(L_{Si,0} - L_{Si})}{dt} = k_1' C_{Si}|_o \qquad (3)$$

with initial condition $L_{Si}=L_{Si,0}$.

The concentration of elemental Si at the surface $C_{Si}|_0$ can be calculated from the continuity equation for Si in the growing layer:

$$\frac{\partial C_{Si}}{\partial t} = D_{Si,eff}\frac{\partial^2 C_{Si}}{\partial x^2} \tag{4}$$

with initial condition $C_{Si}|_{t=0} = C_{Si,bulk}$, and boundary conditions:

$$C_{Si}|_{L(t)} = C_{Si,bulk} \tag{5}$$

$$D_{Si,eff}\frac{\partial C_{Si}}{\partial x}|_o = k_1' C_{Si}|_o \tag{6}$$

where $D_{Si,eff}$ is the effective diffusion coefficient of Si through the growing molybdenum layer ($m^2\ s^{-1}$) and $C_{Si,bulk}$ is the Si concentration in the sample. The first boundary condition simply states that the Si concentration at the Mo/Si interface is equal to the concentration in the substrate, while according to the second boundary condition the flux of Si to the surface is equal to the consumption of Si on that surface.
This model is solved numerically using routine D03PJF from the NAG-library [11], and is coupled to the non-linear regression Marquardt routine [12]. In this routine regression of measured mass increase data to obtain maximum likelihood estimates for $D_{Si,eff}$, k_1' and r_{II} is performed by application of the least square criterion to the observed and calculated mass increases.

3.4 Kinetics of molybdenum deposition from MoF_6 and H_2

Figure 2 shows a typical growth curve together with the growth curve calculated with the model using estimated parameters values. As can be seen the model describes the experiment very well. The net mass increase at t=1500 s is calculated from the slope of the measured curve to be $5.5 \cdot 10^{-3}$ g m^{-2} s^{-1}, while the estimated rate of reaction **r.II**, r_{II}, amounts to $3.5 \cdot 10^{-3}$ g m^{-2} s^{-1}. So the reduction of MoF_6 by Si still accounts for 36 % of the nett overall mass increase after 1500 s and, thus, cannot be neglected. This is also shown in figure 2 by the curve of the contribution of **r.I**.

The effective diffusion coefficient of Si through the layer, $D_{Si,eff}$, varies from one experiment to the other in the range of $6 \cdot 10^{-16}$ -$4 \cdot 10^{-15}$ m^2 s^{-1}; a distinct trend could not be observed. These values are of the same order of magnitude as those used by Joshi *et al.* [6], to describe the non-self-limiting deposition of tungsten by reduction of WF_6 by Si. They compared the CVD of tungsten by reduction of WF_6 by Si in a UHV system with the CVD of tungsten in a commercial LPCVD reactor. The growth of tungsten in both systems appeared to be non-self-limiting, showing a non-linear dependence of the grown layer thickness on time. The films grown in the LPCVD reactor however were much thicker. They also found large oxygen concentrations in the LPCVD grown layers, a gradient of elemental Si throughout the layers, and a density for LPCVD grown tungsten equal to 60-70 % and for UHV grown films equal to 90-100% of the density of bulk tungsten. The grown films were microcrystalline and nonporous. The differences between UHV and LPCVD were attributed to the relatively high levels of water vapour present in the LPCVD reactor, leading to the formation of a fine-grained W structure surrounded by a W-O layer, which assists faster diffusion of Si through the tungsten films compared to the UHV system. So, the results presented in 3.1 and 3.2 are very similar to those presented by Joshi *et al.*, who attributed these to the presence of water contamination in the reactor. It can therefore not be excluded that different background pressures of water vapour in the microbalance setup are responsible for the large range of effective diffusion coefficients found.

The pseudo first order reaction coefficient k_1' was large, ranging from 10^{-8} to 10^{-7} m s^{-1}, compared to the diffusion rate of Si, $D_{Si,eff}/L_{Mo} < 10^{-8}$ m s^{-1} within 60 s, and hardly influenced the regression. As diffusion of Si through the growing layer and reaction of Si with MoF_6 at the gas-solid interface are consecutive steps, the former obviously will become the rate determining step in reaction **r.I**, when the diffusion length of the silicon, L_{Mo}, becomes sufficiently long, typically after one minute.

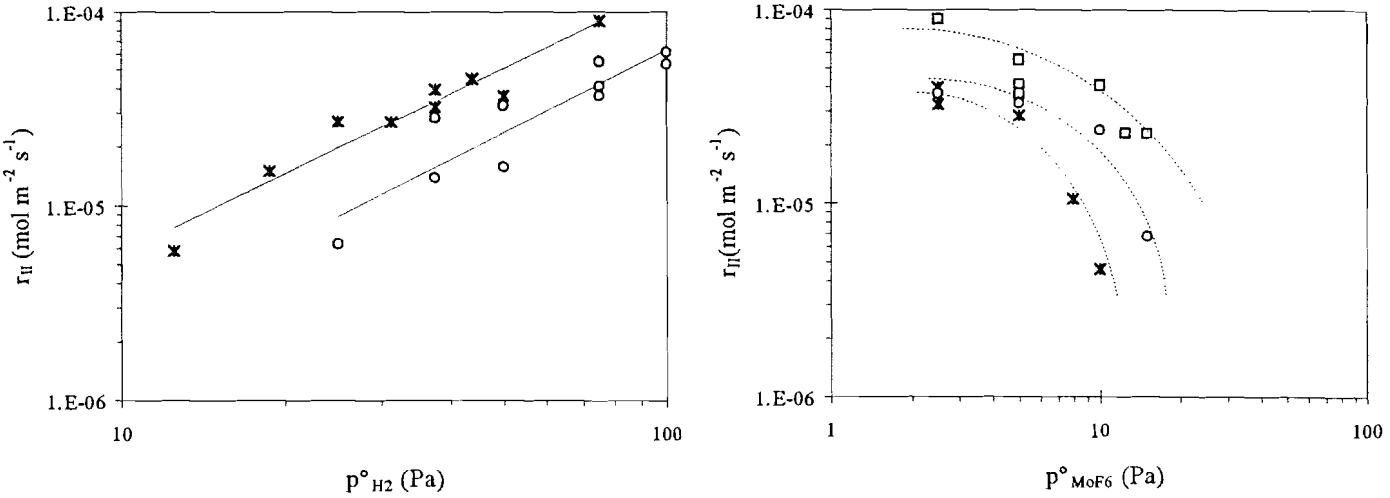

Figure 7 Reaction rate r_{II} as a function of $p°_{H2}$ (a) and $p°_{MoF6}$ (b). **a.** T=600 K; ○ $p°_{MoF6}$=5.0 Pa and * $p°_{MoF6}$=2.5 Pa. **b.** T=600 K, * $p°_{H2}$= 37.5 Pa, ○ $p°_{H2}$= 50.0 Pa and □ $p°_{H2}$= 75.0 Pa.

Figures 7a and 7b show the reaction rate of reduction of MoF_6 by H_2, r_{II}, as a function of the H_2 and MoF_6 partial pressures respectively. The dependency of r_{II} in $p°_{H2}$ corresponds to a partial reaction order of about 1.4, while that in $p°_{MoF6}$ is slightly negative at low $p°_{MoF6}$ and becomes strongly negative at higher $p°_{MoF6}$. The partial reaction orders in $p°_{MoF6}$ are similar to the results reported by Creighton [14], who studied the deposition of tungsten from WF_6 and H_2 using the microbalance technique. Creighton observed a partial reaction order in $p°_{WF6}$ ranging from nearly zero to strongly negative values, and a partial reaction order in $p°_{H2}$ ranging from ½ to values appreciably higher than one. The negative values of the partial reaction order in $p°_{WF6}$ become more pronounced at lower $p°_{H2}$. A simple reaction mechanism based on the Langmuir-Hinshelwood model was used to explain these results. At high $p°_{WF6}$ the surface is believed to be mainly occupied by adsorbed fluorine from WF_x, which inhibites chemisorption of H_2. Dissociative adsorption of H_2 then becomes the rate determining step, leading to a first order dependence in $p°_{H2}$ and a minus one order in $p°_{WF6}$. At sufficiently high $p°_{H2}$ the dependency in $p°_{H2}$ is expected to become negative, while the deposition rate will show a first order dependence in $p°_{WF6}$, according to the proposed mechanism. Ammerlaan [15] suggests that the mechanisms proposed by McConica and Krishnamani [7], and by Pauleau and Lami [16] may even lead to partial reaction orders in $p°_{WF6}$ as low as minus two at low $p°_{H2}$. In addition etching of tungsten by WF_6 can account for deviations in the observed orders at low $p°_{H2}$ [14].

The partial reaction orders in the present work are not consistent with the partial reaction orders of ½ in $p°_{H2}$ and 0 in $p°_{MoF6}$ reported by Sahin *et al.* [5]. A possible explanation for these differences is that Sahin *et al.* used a cold wall reactor for their deposition experiments in which transport phenomena, like thermal diffusion, can easily obscure intrinsic kinetics [13]. Thermal diffusion causes heavy species like MoF_6 to diffuse away from the heated wafer surface, leading to a significant lower $p°_{MoF6}$ above the substrate. Therefore the actual conditions above the reacting surface can easily shift towards higher p_{H2}/p_{MoF6} ratios then the ratio at the inlet of the reactor. According to the mechanisms mentioned above a higher order in $p°_{MoF6}$ and a lower order in $p°_{H2}$ can then be expected.

5. CONCLUSIONS

A microbalance setup was used to study the kinetics of molybdenum deposition on silicon from MoF_6 and H_2. The significant contribution of the reaction of MoF_6 with Si to the overall molybdenum deposition rate obscures the intrinsic kinetics of the reduction of MoF_6 by H_2. In order to separate both reaction pathways, a model was developed taking into account diffusion of Si through the growing layer. Integrating numerically the model and applying a non-linear regression a partial reaction order of 1.4 in hydrogen was found for the reduction of MoF_6 by H_2. The order in MoF_6 for this reaction is negative.

REFERENCES

[1] Lifshitz N. and Green M.L., *J. Electrochem. Soc.*, **135** (1988) 131-136.

[2] Lifshitz N., Williams D.S., Capio C.D. and Brown J.M., *J. Electrochem. Soc.*, **134** (1987) 2061-2067.

[3] Woodruff D.W. and Sanchez-Martinez R.A., "CVD Molybdenum from MoF_6", Tungsten and Other Refractory Metals for VLSI Applications II, 1986, E.K. Broadbent Ed. (Materials Research Society, Pittsburgh, PA 1987) pp. 207-213.

[4] Sahin T. and Park C.-S.,"Low Pressure Chemical Vapour Deposition of Molybdenum by Silicon Reduction of MoF_6", Tungsten and Other Refractory Metals for VLSI Applications IV, 1988, R.S. Blewer and C.M. McConica Eds. (Materials Research Society, Pittsburgh, PA 1989) pp. 253-256.

[5] Sahin T., Flanigan E.J. and Sears J.T., "Low Pressure Chemical Vapour Deposition of Molybdenum: 1. Kinetics and Reaction Mechanisms", Tungsten and Other Refractory Metals for VLSI Applications II, 1986, E.K. Broadbent Ed. (Materials Research Society, Pittsburgh, PA 1987) pp. 199-205.

[6] Joshi R.V., Prasad V., Yu M.L., Scilla G., *J. Appl. Phys.*, **71** (1992) 1428-1441.

[7] Broadbent E.K., Ramiller C.L., *J. Electrochem. Soc.*, **131** (1984) 1427-1433.

[8] McConica C.M. and Krishnamani K., *J. Electrochem. Soc.*, **133** (1986) 2542-2548.

[9] Weerts W.L.M., "Low Pressure CVD of Polycrystalline Silicon: Reaction Kinetics and Reactor Modelling", Ph. D. Thesis, University of Technology Eindhoven, Eindhoven, to be published, 1995.

[10] David R. and Matras D., *Can. J. Chem. Eng.*, **53** (1975) 297-300.

[11] NAG Ltd, Fortran Library Manual, # 15, (Wilkinson House, Oxford, 1991).

[12] Marquardt D.W., *J. Soc. Indust. Appl. Math.*, **11** (1963) 431-441.

[13] Kleijn, C.R., "Transport Phenomena in Chemical Vapor Deposition reactors", Ph. D. Thesis, Delft University of Technology, Delft, 1991.

[14] Creighton J.R., *Thin solid films*, **24** (1994) 310-317.

[15] Ammerlaan J.A.M., "Kinetics and Characterization of Tungsten CVD Processes", Ph. D. Thesis, Delft University of Technology, Delft, 1994.

[16] Pauleau Y. and Lami Ph., *J. Electrochem. Soc.*, **132** (1985) 2779-2784.